Ministry of Education and Science of Ukraine

ODESSA NATIONAL ACADEMY OF FOOD TECHNOLOGIES

International Competition of Student Scientific Works

BLACK SEA SCIENCE 2020

PROCEEDINGS

ODESSA, ONAFT 2020

Ministry of Education and Science of Ukraine

Odessa National Academy of Food Technologies

International Competition of Student Scientific Works

BLACK SEA SCIENCE 2020

Proceedings

Odessa, ONAFT 2020

UDC 001.8(063)

Black Sea Science 2020: Proceedings of the International Competition of Student Scientific Works / Odessa National Academy of Food Technologies; B. Yegorov, M. Mardar (editors-in-chief.) [*et al.*]. – Odessa: ONAFT, 2020. – 621 p.

Proceedings of International Competition of Student Scientific Works «Black Sea Science 2020» contain the works of winners of the competition.

The author of the work is responsible for the accuracy of the information.

Organizing committee:

Prof. Bogdan Iegorov, D.Sc., Rector of Odessa National Academy of Food Technologies, Head of the Committee

Prof. Maryna Mardar, D.Sc., Vice-Rector for Scientific and Pedagogical Work and International Relations of Odessa National Academy of Food Technologies, Deputy Head of the Committee

Prof. Stefan Dragoev, D.Sc., Vice-Rector for Scientific Work and Business Partnerships of University of Food Technologies (Bulgaria)

Prof. Baurzhan Nurakhmetov, D.Sc., First Vice-Rector of Almaty Technological University (Kazakhstan)

Prof. Mircea Bernic, Dr. habil., Vice-Rector for Scientific Work of Technical University of Moldova (Moldova)

Prof. Jacek Wrobel, Dr. habil., Rector of West Pomeranian University of Technology (Poland)

Prof. Michael Zinigrad, D.Sc., Rector of Ariel University (Israel)

Dr. Mei Lehe, Ph.D., Vice-President of Ningbo Institute of Technology, Zhejiang University (China)

Prof. Plamen Kangalov, Ph.D., Vice-Rector for Academic Affairs of “Angel Kanchev” University of Ruse (Bulgaria)

Dr. Alexander Sychev, Ph.D., Assoc. Professor of Sukhoi State Technical University of Gomel (Belarus)

Dr. Hanna Lilishentseva, Ph.D., Assoc. Professor, Head of the Department of Merchandise of Foodstuff of Belarus State Economic University (Belarus)

Prof. Heinz Leuenberger, Ph.D., Professor of the Institute of Ecopreneurship of University of Applied Sciences and Arts (Switzerland)

Prof. Edward Pospiech, Dr. habil., Professor of the Institute of Meat Technology of Poznan University of Life Sciences (Poland)

Prof. Lali Elanidze, Ph.D., Professor of the Faculty of Agrarian Sciences of Iakob Gogebashvili Telavi State University (Georgia)

Dr. V. Kozhevnikova, Ph.D., Senior Lecturer of the Department of Hotel and Catering Business of Odessa National Academy of Food Technologies, Secretary of the Committee

4. POWER ENGINEERING AND ENERGY EFFICIENCY

DETERMINATION OF RATIONAL GEOMETRICAL RELATIONS OF SINGLE-PHASE ELECTROMAGNETIC SYSTEMS WITH RECTANGULAR CROSS SECTIONS OF RODS

Author: Churilo Ruslan
Supervisor: Sadovoy Aleksey
Mykolaiv National Agrarian University (Ukraine)

Abstract. *Determination and comparison of TLI variants of traditional ISD with a rod EMS having a rectangular section of the rods and different methods for making the magnetic circuit.*

The numerical comparison of the TLI variants of ST electromagnetic systems with twisted and charged magnetic circuits, on the basis of the principle of electromagnetic equivalence and the development of design mathematical models of transformers is carried out.

The analysis is carried out at different voltage classes K_f = 0.2 ... 0.3, ratios of specific active materials (coil copper and ETS) $\gamma_o / \gamma_c = 8{,}9/7{,}65$, *as well as their values in the range C_o / C_c = 3,0 ... 5,5.*

Key words*: single-phase transformer and reactor, twisted and charged magnet conductor, mass indexes, optimization, controlled variables.*

1. INTRODUCTION

For more than 100 years, the designs of inductive static devices (ISD) electromagnetic systems (EMS) of small and medium power have practically not changed. All single-phase transformers (ST) and single-phase reactors (SR) of the specified power have rectangular "traditional" forming contours (FK), which are manufactured in different ways. ISD magnetic leads are made of electrotechnical steel (ETS) by charging, winding or bending of strips [1-7].

In connection with the mass release of ST and SR of small and medium power, both with the charged and with the twisted magnet, the question arises of their rational choice based on the numerical comparative analysis of technical level indicators (TLI) results.

The goal of the work. Determination and comparison of TLI variants of traditional ISD with a rod EMS having a rectangular section of the rods and a different methods for making the magnetic circuit.

2. PREVIOUS STUDIES OF SINGLE-PHASE ROD TRANSFORMERS ANALYSIS

The introduction shows the need to develop an optimal benchmarking method for selecting ISD based on their own characteristics. According to the results of the survey, in [12, 13] the problem of comparative analysis of EMS was considered, but general recommendations for the relations of the geometric dimensions of the magnetic core and graphic dependences were determined.

In these papers [10-12], according to the optimization criterion, a minimum of one of the specific TLI was taken - the mass, volume or value of the EMS per unit of power of the ISD. The applied dimensionless geometric controlled variables (CV) *l*, *m*, *n* are the ratios, respectively, of the rectangular section of the rod *b*, the height *h* and the width *c* of the winding window to the section of the rod width *a*:

$$l = b/a;\ m = h/a; n = c/a. \tag{1}$$

On the basis of equations (1) we obtain practical, analytical, geometric dependences for choosing the optimal geometric relations for the above criteria for EMS structures.

According to [12, 13], the methods of calculating one-and three-phase transformers with rectangular cross sections of the cores of the magnetic circuits contain inaccuracies and errors, and there are no methods that allow the evaluation of the technical parameters of the ISD at the stage of the choice of the principal structure, that is, the methods of structural synthesis of these devices. It is shown the possibility of optimizing transformers with the use of common target functions (TF) and dimensionless (relative) CV (1) is proposed in [10]. It is determined that for all EMS structures with rectangular generating contours, the optimal ratio of the sides of the cross-section of the rod is close to two, and the ratio of the sides of the window is more than two. However, numerical results of the optimization comparison of single-phase electromagnetic loading (EML) of variants in [13], as in [11, 12], are absent.

The question of determining the optimal geometric ratios of traditional single-phase EMS is also considered in [8], where the TF and graphic dependences of the determination of optimal geometric relations of traditional EMS are presented. Similar analogous (1) relative geometric CV are used. For all traditional EMS structures, the ranges of optimal geometric ratios of main dimensions of the magnetic conductors.are obtained. However, there is no analytical comparison (the meaning and difference of the technical level indicators) of the EMS variants in [8], as in [10-13].

2.1 Method of electromagnetic systems comparative analysis

The determination and comparison of the TLI of the EMS variants is possible on the basis of the principle of electromagnetic equivalence, as well as in the design of the design mathematical models (MM) with the private and integral optimization criteria containing universal (identical for each construction) relative CV [2,3] . Such a position corresponds to the MM method with integral functions containing optimization components with universal geometric and electromagnetic variables [6].

$$F_{kii} = \mathrm{K}_{\mathrm{tii}} \left(\sqrt[4]{\mathrm{P}_{\mathrm{sd}}}\right)^3 \cdot \mathrm{P}^*_{kii}, \tag{2}$$

where P_{sd} – index of source data and EML; $\mathrm{K}_{\mathrm{tii}}$ – component of specific indicators of used materials К ≥ 3 of TF – private optimization criteria; P^*_{kii} – a dimensionless optimization component that characterizes each of the *i*-CV, the main of which are the functions of the mass P_{1ii}, the cost P_{2ii} and the loss of the active power P_{3ii} of the ii version of the EMS.

Extremes P*kii of dimensionless components of the TF (2) are TLI ISD. Each of the P_{kii}* depends on the form of filling form the winding window with the conductive material of windings coils (voltage class) K_f and two identical and acceptable for any of the available and possible versions of the EMS CV - the ratio a_m of the outer diameter D_{1ii} and the internal diameter D_{2ii} of the calculated circles of the magnetic circuit for each *ii* EMS variant, the ratios λ_0 of height h_{0ii} and the width b_{0ii} of the winding window and the main angle of the rod α_c [5, 6]:

$$\text{P}_{1(2)ii} = f\left(\text{K}_\text{f}, a_m, \lambda_0, \alpha_\text{c}\right); \quad (3)$$

$$a_m = {D_{1ii}} / {D_{2ii}}; \quad (4)$$

$$\lambda_0 = {h_{0ii}} / {b_{0ii}}, \quad (5)$$

where K_f – the filling the winding window coefficient, taking into account the voltage class is used in the part of EMS; a_m and λ_0 – geometric relative CV; α_c – the main angle of the rod;

The component of K_{tii} of the target function (2) includes, depending on the optimization criterion, the ratio of the specific densities of materials (coil copper and ETS) (kg / m3) and their values C_o/C_c = 3,0 ... 5,5, the coefficients of stacking K_c = 1 , 13 and an excitation K_e = 1.15 turns of coils at impregnation [2], contour coefficient, $\text{K}_\text{k} = 1$. The calculations are performed at different K_f = 0,2 ... 0,3 and the ratios of the specific values of the active materials in the range $\text{C}_\text{c}/\text{C}_\text{o} = 3{,}0\ldots5{,}5$.

In modern ST and SR used anisotropic ETS grades 3406-3409 with $\text{K}_{\text{зс}} = 0{,}96 - 0{,}97$ at the thickness of the tape (roll, plate) $\delta_\text{c} = 0{,}27 - 0{,}35$ mm. At f1 = 50 Hz, in ranges $S_н = 0{,}3 - 1\,\text{кВ}\cdot\text{А}$ and $S_н = 1 - 2{,}5\,\text{кВ}\cdot\text{А}$ respectively $J_0 = 2{,}4 - 1{,}7\ \text{А/мм}^2$ and $J_0 = 1{,}7 - 2{,}4\ \text{А/мм}^2$ [13].

In the comparative analysis of the considered variants in accordance with the principle of electromagnetic equivalence [5], respectively, the same materials used, the density of currents of windings, the mean values of the magnetic field induction amplitudes in the rods and yards, and also the execution and methods of cooling the ISD are taken.

3. DEVELOPMENT OF SINGLE-PHASE TRANSFORMERS MATHEMATICAL MODELS

3.1 Mathematical models development of mass and cost of a basic electromagnetic system with a twisted magnetic circuit

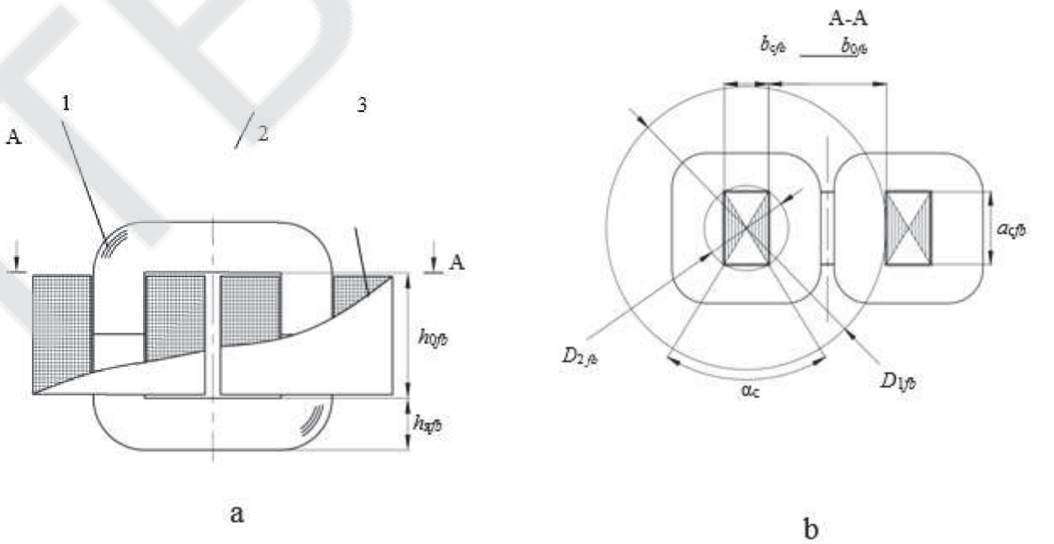

Fig. 1 - Constructive scheme (a) and design diameters (b) of planar EMS with a rectangular winding window and sections of the rods of the twisted magnet circuit: 1 – rod; 2 – yoke; 3 – winding.

The first controlled change of the TF of basic rod EMS with rectangular FC MM (Fig. 1)

$$a_m = D_{1fb} / D_{2fb}\,, \tag{6}$$

where D_{1fb}, D_{2fb},, – outer diameter and internal diameter of calculated circles of the magnetic circuit, respectively.

Second controlled change in the MM EMS (Fig. 1)

$$\lambda_0 = h_{0fb} / b_{0fb}\,, \tag{7}$$

where h_{0fb} and $b_{0\,fb}$ – winding window height and width of the base magnetic EMS.

The values of the sides of the a_{cfb} and b_{cfb} of the rod section (Fig. 1) are determined by D_{2fb}, and the center angle of the rod α_c:

$$a_{c\,fb} = D_{2fb} \sin(\alpha_c/2); \tag{8}$$

$$b_{c\,fb} = D_{2fb} \cos(\alpha_c/2). \tag{9}$$

The area of the ETS of the magnetic circuit rods of the EMs (Fig. 1), is determined taking into account (8) and (9)

$$S_{c\,fb} = K_{3c} a_{c\,fb} b_{c\,fb} = K_{3c} D_{2fb}^{\;2} \sin(\alpha_c)/2. \tag{10}$$

The width of winding windows b_{0fb} (Fig. 1) depends on D_{2fb}, a_m and (9)

$$b_{0fb} = D_{2fb}/2 - b_{c\,fb}/2 = D_{2fb}/2\left(a_m - \sin(\alpha_c/2)\right). \tag{11}$$

The ETS mass of the EMs magnetic circuit is determined using (7), (8) and (9)

$$m_{mfb} = K_{3c}\gamma_c\left(2h_{0fb}S_{c\,fb} + 2b_{0fb}S_{c\,fb} + \pi S_{c\,fb}b_{c\,fb}\right) =$$
$$= 0{,}5K_{3c}\gamma_c D_{2fb}^3 \sin\alpha_c\left(\left(a_{\text{м}} - \sin(\alpha_c/2)\right)(\lambda_0 + 1) + \pi\sin(\alpha_c/2)\right). \tag{12}$$

On the basis of (10) and (11) we obtain the basic equations of the EMS variants (Fig. 1) and the connections S_{cfb} and b_{0fb}

$$S_{c\,fb} = P_{sd}/\left(S_{0fb}K_f\right) = P_{sd}/\left(b_{0fb}^2\lambda_{0fb}K_f\right) = 4P_{sd}/\left(D_{2fb}^2\lambda_{0fb}\left(\sin(\alpha_c/2)\right)^2 K_f\right), \tag{13}$$

where S_{0fb} – area of the winding window EMS (Fig.1),

$$S_{0fb} = h_{0fb}b_{0fb}K_f = b_{0fb}^2\lambda_{0fb}K_f\,, \tag{14}$$

From equation (10) and (13) follows:

$$K_{3c}\,D_{2fb}^2 \sin(\alpha_c)/2 = 4P_{sd}/D_{2fb}^2\lambda_{0fb}\left(a_m - \sin(\alpha_c/2)\right)^2 K_f\,;$$

$$D_{2fb} = \sqrt[4]{8P_{sd}/\left(K_f K_{3c}\lambda_0 \sin(\alpha_c)\left(a_m - \sin(\alpha_c/2)\right)^2\right)}. \tag{15}$$

After substituting equations (15) into (12), the expression for finding the mass of the ETS of the magnetic circuit EMC (Fig. 1):

$$m_{mfb} = 0{,}5K_{3c}\gamma_c \sin\alpha_c\left(\sqrt[4]{8P_{sd}/\left(K_f K_{3c}\lambda_0 \sin(\alpha_c)\left(a_m - \sin(\alpha_c/2)\right)^2\right)}\right)^3 \times$$
$$\times\left(\left(a_m - \sin(\alpha_c/2)\right)(\lambda_0 + 1) + \pi\sin(\alpha_c/2)\right) = \gamma_c\left(\sqrt[4]{P_{sd}}\right)^3 P_{mfb}^*. \tag{16}$$

where P_{mfb}^* – relative mass index of the magnetic circuit (Fig. 1),

$$P^*_{mfb} = 0{,}5K_{зс}\sin\alpha_c\left(\sqrt[4]{8P_{sd}/\left(K_f K_{зс}\lambda_0 \sin(\alpha_c)(a_m - \sin(\alpha_c/2))^2\right)}\right)^3 \times$$

$$\times\left((a_m - \sin(\alpha_c/2))(\lambda_0 + 1) + \pi\sin(\alpha_c/2)\right). \quad (17)$$

The average length of the coil rope for the rod EMS (Fig. 1) is determined on the basis of (8), (9) and (11):

$$l_{wfb} = 2(a_{cfb} + b_{cfb}) + \pi b_{0fb}/2 = D_{2fb}\left(\sin(\alpha_c/2) + \cos(\alpha_c/2) + \frac{\pi}{8}(a_m - \sin(\alpha_c/2))\right). \quad (18)$$

Substituting (11) in (18) we obtain the mass equation of copper winding for EMS:

$$m_{ofb} = \gamma_o K_в K_y K_f D^3_{2fb}\lambda_0 0{,}5(a_m - \sin(\alpha_c/2))^2\left((\sin(\alpha_c/2) + \cos(\alpha_c/2))\right) +$$

$$+ \pi(a_m - \sin(\alpha_c/2))/8 \quad (19)$$

Substitution of equation (15) transforms (19):

$$m_{ofb} = \gamma_o K_в K_y K_f\left(\sqrt[4]{8P_{sd}/\left(K_f K_{зс}\lambda_0 \sin(\alpha_c)(a_m - \sin(\alpha_c/2))^2\right)}\right)^3 0{,}5\lambda_0(a_m - \sin(\alpha_c/2))^2 \times$$

$$\times\left((\sin(\alpha_c/2) + \cos(\alpha_c/2))\right) + \pi(a_m - \sin(\alpha_c/2))/8 = \gamma_o\left(\sqrt[4]{P_{sd}}\right)^3 P^*_{ofb}, \quad (20)$$

where P^*_{ofb} - relative mass index of active materials of the EMS winding (Fig. 1).

$$P^*_{ofb} = \gamma_o K_в K_y K_f\left(\sqrt[4]{8/\left(K_f K_{зс}\lambda_0 \sin(\alpha_c)(a_m - \sin(\alpha_c/2))^2\right)}\right)^3 0{,}5\lambda_0(a_m - \sin(\alpha_c/2))^2 \times$$

$$\times\left((\sin(\alpha_c/2) + \cos(\alpha_c/2))\right) + \frac{\pi}{8}(a_m - \sin(\alpha_c/2)). \quad (21)$$

The weight m_{afb} and cost C_{afb} of EMS active materials (Fig. 1) are determined on the basis of (16) and (20):

$$m_{afb} = m_{mfb} + m_{ofb} = \gamma_c\left(\sqrt[4]{P_{sd}}\right)^3 P^*_{mfb} + \gamma_o\left(\sqrt[4]{P_{sd}}\right)^3 P^*_{ofb} = \gamma_c\left(\sqrt[4]{P_{sd}}\right)^3 P^*_{1fb}; \quad (22)$$

$$C_{afb} = C_{mfb} + C_{ofb} = \gamma_c C_c\left(\sqrt[4]{P_{sd}}\right)^3 P^*_{mfb} + \gamma_o C_o\left(\sqrt[4]{P_{sd}}\right)^3 P^*_{ofb} = \gamma_c\left(\sqrt[4]{P_{sd}}\right)^3 P^*_{2fb} \quad (23)$$

where P^*_{1fb} and P^*_{2fb} relative indicators of mass and cost of planar (Fig. 1), with rectangular rods of twisted magnetic circuits:

$$P^*_{1fb} = \left(\sqrt[4]{8/\left(K_f K_{зс}\lambda_0 \sin(\alpha_c)((a_m - \sin(\alpha_c/2)))^2\right)}\right)^3 \times$$

$$\times\left(K_{зс}0{,}5\sin\alpha(a_m - \sin(\alpha_c/2))(\lambda_0 + 1) + \pi\sin(\alpha_c/2) + (\gamma_o/\gamma_c)K_в K_y K_f \times\right.$$

$$\left.\times 0{,}5\lambda_0(a_m - \sin(\alpha_c/2))^2(\sin(\alpha_c/2) + \cos(\alpha_c/2)) + \pi(a_m - \sin(\alpha_c/2))/8\right); \quad (24)$$

Extremes (minima) P^*_{1fb} of indicators (24) obtained for three values K_f in Annex 1 (Table 1).

$$P^{*}_{2fb} = \left(\sqrt[4]{8/\left(K_f K_{3c}\lambda_0 \sin(\alpha_c)\left(\left(a_m - \sin(\alpha_c/2)\right)\right)^2\right)}\right)^3 \times$$
$$\times\left(K_{3c} 0{,}5\sin\alpha_c\left(a_m - \sin(\alpha_c/2)\right)(\lambda_0 + 1) + \pi\sin(\alpha_c/2) + \left(C_o\gamma_o/C_c\gamma_c\right)K_в K_y K_f \times\right.$$
$$\times 0{,}5\left(a_m - \sin(\alpha_c/2)\right)^2\left(\sin(\alpha_c/2) + \cos(\alpha_c/2)\right) + \pi\left(a_m - \sin(\alpha_c/2)\right)/8; \quad (25)$$

Extremes (minima) P^{*}_{2fb} of indicators (25) obtained for three values K_f in Annex 1 (Table 2).

3.2 Mathematical models development of mass and cost of a rod electromagnetic system with a charged magnet wire

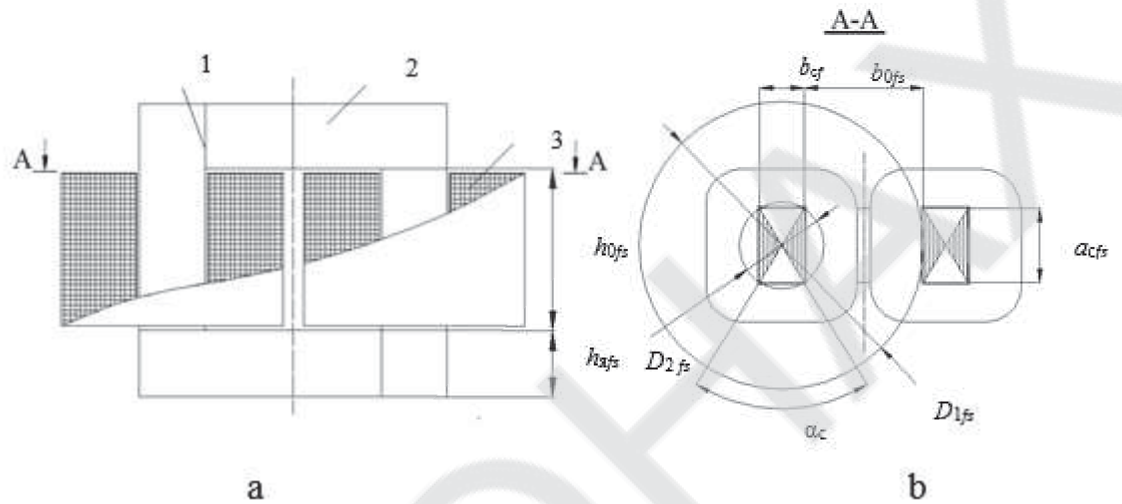

Fig. 2 - Constructive scheme (a) and design diameters (b) planar EMS with a rectangular winding window and sections of the magnetic core: 1 – rod; 2 – yoke; 3 – winding

First CV TF MM of base rod EMS with rectangular CK, are determined accordingly (4)

$$a_m = D_{1sf}/D_{2sf}\ , \quad (49)$$

where D_{1sf}, D_{2sf} – outer diameter and internal diameter of calculated circles of the magnetic circuit, respectively;

Second CV TF EMS determined by the (5)

$$\lambda_0 = h_{0sf}/b_{0sf}\ , \quad (50)$$

where h_{0sf}, and b_{0sf} – winding window height and width of the base magnetic EMS..

The values of the sides of the a_{csf} and b_{csf} of the rod section (Fig. 1) are determined by D_{2sf}, and the center angle of the rod α_c:

$$a_{csf} = D_{2sf}\cos(\alpha_c/2); \quad (51)$$

$$b_{csf} = D_{2sf}\sin(\alpha_c/2). \quad (52)$$

The area of the ETS magnetic circuit rods EMS, determined by taking into account the size of the sides a_{csf} and b_{csf} the cross-section of the rod

$$S_{csf} = K_{3c} a_{csf} b_{csf} = K_{3c} D_{2sf}^{\ 2}\sin(\alpha_c)/2. \quad (53)$$

The width of each of the winding windows b_{0sf}, depends on D_{2sf}, a_m and the side of the rod section b_{csf}

$$b_{0sf} = D_{2sf}/2 - b_{csf}/2 = D_{2sf}/2\left(a_m - \sin(\alpha_c/2)\right). \quad (54)$$

The mass of the ETS of the magnetic circuit of the EMS is determined using the second CV MM EMS, and the values of the sides a_{csf} and b_{csf} are the cross-section of the rod

$$m_{msf} = K_{3c}\gamma_c D_{2sf}^3 \sin\alpha\left[\left(a_m - \sin(\alpha_c/2)\lambda_o \cdot 0{,}5 + \left(a_m - \sin(\alpha_c/2)\cdot 0{,}5 + 2\sin(\alpha_c/2)\right]\right.\right..$$

(55)

Based on ETS area of the magnetic circuit rods S_{csf} and the widths of each winding window b_{0sf} we obtain the basic equations of the EMS variants and the connections S_{csf} and b_{0sf}

$$S_{csf} = P_{sd}/\left(S_{0sf}\,K_f\right) = P_{sd}/\left(b_{0sf}^2\lambda_o K_f\right) = 4P_{sd}/\left(D_{2sf}^2\,\lambda_0\left(\sin(\alpha_c/2)\right)^2 K_f\right), \quad (56)$$

where S_{0sf} – area of the winding window EMS

$$S_{0sf} = h_{0sf} b_{0sf}\,K_f = b_{0sf}^2\,\lambda_0 K_f\,, \quad (57)$$

From the equality of equations (53) and (58) follows:

$$K_{3c} D_{2sf}^2\,\sin\alpha_c/2 = 4P_{sd}\Big/D_{2\,fb}^2\lambda_0\left(a_m - \sin(\alpha_c/2)\right)^2 K_f\;;$$

$$D_{2sf} = \sqrt[4]{8P_{sd}\Big/\left(K_f K_{3c}\lambda_0\,\sin(\alpha_c)\left(a_m - \sin(\alpha_c/2)\right)^2\right)} \quad (58)$$

After substituting equations (58) into (55), the expression of finding the mass of the ETS magnetic circuit EMS will have the form

$$m_{msf} = K_{3c}\gamma_c\left(\sqrt[4]{8\cdot P_{sd}\Big/\left(K_f K_{3c}\lambda_o\,\sin(\alpha_c)\left(a_m - \sin(\alpha_c/2)\right)^2\right)}\right)^3 \times$$

$$\times\sin\alpha\left[\left(a_m - \sin(\alpha_c/2)\right)\lambda_o\cdot 0{,}5 + \left(a_m - \sin(\alpha_c/2)\right)\cdot 0{,}5 + 2\sin(\alpha_c/2)\right] = \gamma_c\left(\sqrt[4]{P_{sd}}\right)^3\cdot P_{msf}^*\,, \quad (59)$$

where P_{msf}^* – relative mass index of the magnetic circuit

$$P_{msf}^* = K_{3c}\sin\alpha_c\left(\sqrt[4]{8P_{sd}\Big/\left(K_f K_{3c}\lambda_0\,\sin(\alpha_c)\left(a_m - \sin\alpha_c/2\right)^2\right)}\right)^3 \times$$

$$\times\sin\alpha\left[\left(a_m - \sin(\alpha_c/2)\right)\lambda_o\cdot 0{,}5 + \left(a_m - \sin(\alpha_c/2)\right)\cdot 0{,}5 + 2\sin(\alpha_c/2)\right]. \quad (60)$$

The average length of the coil rope for the rod EMS is determined on the basis of (51), (52) and (54):

$$l_{sf} = D_{2sf}\left(2\cos(\alpha_c/2) + 2\sin(\alpha_c/2) + (\pi/8)\left(a_m - \sin(\alpha_c/2)\right)\right). \quad (61)$$

Substituting (54) into (61) we obtain the mass equation of copper winding for EMS:

$$m_{osf} = \gamma_o K_в K_y K_f \lambda_o D_{2sf}^3\left[0{,}25\left(a_m - \sin(\alpha_c/2)\right)^2 \times\right.$$

$$\left.\left[2\cos(\alpha_c/2) + 2\sin(\alpha_c/2) + \pi/8\left(a_m - \sin(\alpha_c/2)\right)\right]\right] \quad (62)$$

Substitution (58) transforms (62)

$$m_{osf} = \gamma_o K_в K_y K_f \lambda_o\left(\sqrt[4]{8P_{sd}\Big/\left(K_f K_{3c}\lambda_o\,\sin\alpha_c\left(a_m - \sin(\alpha_c/2)\right)^2\right)}\right)^3\cdot\left[0{,}25\left(a_m - \sin(\alpha_c/2)\right)^2 \times\right.$$

$$\times\left[2\cos(\alpha_c/2)+2\sin(\alpha_c/2)+(\pi/8)\left(a_m-\sin(\alpha_c/2)\right)\right]\Big]=\gamma_o\left(\sqrt[4]{\mathrm{P_{sd}}}\right)^3\cdot \mathrm{P}^*_{osf}\,, \qquad (63)$$

where P^*_{osf} – relative mass index of active materials of the EMC winding:

$$\mathrm{P}^*_{osf}=\gamma_o\mathrm{K_в K_у K_f}\lambda_o\left(\sqrt[4]{8\mathrm{P_{sd}}\Big/\left(\mathrm{K_f K_{зс}}\lambda_o\sin\alpha_c\left(a_m-\sin(\alpha_c/2)\right)^2\right)}\right)^3\times$$

$$\times\left[0{,}25\left(a_m-\sin(\alpha_c/2)\right)^2\left[2\cos(\alpha_c/2)+2\sin(\alpha_c/2)+\pi/8\left(a_m-\sin(\alpha_c/2)\right)\right]\right]. \qquad (64)$$

Mass m_{asf} and cost C_{asf} of active EMS materials are determined on the basis of (59) and (63) equations:

$$m_{asf}=m_{msf}+m_{osf}=\gamma_c\left(\sqrt[4]{\mathrm{P_{sd}}}\right)^3\mathrm{P}^*_{msf}+\gamma_o\left(\sqrt[4]{\mathrm{P_{sd}}}\right)^3\mathrm{P}^*_{osf}=\gamma_c\left(\sqrt[4]{\mathrm{P_{sd}}}\right)^3\mathrm{P}^*_{1sf}\,, \qquad (65)$$

$$C_{asf}=C_{msf}+C_{osf}=\gamma_c C_{csf}\left(\sqrt[4]{\mathrm{P_{sd}}}\right)^3\mathrm{P}^*_{msf}+\gamma_o C_{osf}\left(\sqrt[4]{\mathrm{P_{sd}}}\right)^3\mathrm{P}^*_{osf}=\gamma_c\left(\sqrt[4]{\mathrm{P_{sd}}}\right)^3\mathrm{P}^*_{2sf}\,, \qquad (66)$$

where P^*_{1sf} and P^*_{2sf} relative indicators of mass and cost of planar, with rectangular cores of charged magnetic conduits:

$$\mathrm{P}^*_{1sf}=\sqrt[4]{\frac{8}{\sin\alpha\cdot\mathrm{K_{зс}K_f}\lambda_o\cdot\left(a_m-\sin(\alpha_c/2)\right)^2}}\cdot\Big[\mathrm{K_{зс}}\sin\alpha_c\Big(\left(a_m-\sin(\alpha_c/2)\right)\cdot\lambda_o 0{,}5+$$

$$+\left(a_m-\sin(\alpha_c/2)\right)\cdot 0{,}5+2\sin(\alpha_c/2)\Big)+\left(\gamma_o/\gamma_c\right)\mathrm{K_f K_у K_в}\lambda_o\cdot\Big[0{,}25\left(a_m-\sin(\alpha_c/2)\right)^2\times$$

$$\times\left[2\cos(\alpha_c/2)+2\sin(\alpha_c/2)+\pi/8\left(a_m-\sin(\alpha_c/2)\right)\right]\Big]\Big]; \qquad (67)$$

Extremes (minima) Π^*_{1sf} of indicators (67) obtained for three values K_f in Annex 2 (Table 3).

$$\mathrm{P}^*_{2sf}=\sqrt[4]{\frac{8}{\sin\alpha\cdot\mathrm{K_{зс}K_f}\lambda_o\cdot\left(a_m-\sin(\alpha_c/2)\right)^2}}\cdot\Big[\mathrm{K_{зс}}\sin\alpha_c\Big(\left(a_m-\sin(\alpha_c/2)\right)\cdot\lambda_o 0{,}5+$$

$$+\left(a_m-\sin(\alpha_c/2)\right)\cdot 0{,}5+2\sin(\alpha_c/2)\Big)+\left(\mathrm{C}_{osf}\gamma_o/\mathrm{C}_{osf}\gamma_c\right)\mathrm{K_f K_у K_в}\lambda_o\cdot 0{,}25\left(a_m-\sin(\alpha_c/2)\right)^2\times$$

$$\times\left[2\cos(\alpha_c/2)+2\sin(\alpha_c/2)+\pi/8\left(a_m-\sin(\alpha_c/2)\right)\right]\Big]\Big]. \qquad (68)$$

Extremes (minima) Π^*_{2sf} of indicators (68) obtained for three values K_f in Annex 2 (Table 4).

4. TECHNICAL LEVEL COMPARISON OF ELECTROMAGNETIC SYSTEMS VARIANTS OF SINGLE-PHASE TRANSFORMERS WITH TWISTED AND CHARGED MAGNET CIRCUIT

The results of electromagnetic systems comparative analysis are characterized by PTR comparison of transformers with twisted and charged magnetic circuits according to separate criteria of minimum masses and values. According to [16], a basic transformer with a rod EMC, which has a charged magnetic circuit, was selected in the baseline for comparing the TLI. The results of changes in these indicators are shown in Table. 5

Table 5 - Numerical values of the advantages of technical level indicators of single-phase electromagnetic systems with wired and charged magnetic circuits

Ratio of indicators P^*_{fb} / P^*_{fs}	The range of changes in relation values,%					
	Mass index	Cost Indicator				
		3,5	4	4,5	5	5,5
$K_f = 0{,}2$	-2,656 %	-3,569 %	-3,663 %	-3,742 %	-3,815 %	-3,877 %
$K_f = 0{,}25$	-2,822 %	-3,723 %	-3,813 %	-3,891 %	-3,959 %	-4,021 %
$K_f = 0{,}3$	-2,957 %	-3,846 %	-3,934 %	-4,008 %	-4,076 %	-4,134 %

Note * "-" Improvement of the TLI.

The results of calculations (Table 5) are graphically explained (Figures 3-6), which are given in Annex 3, and show a numerical comparison of the mass values in the EMS with wired and charged magnetic circuits. From Fig. 3-6 it follows that when the coefficient of filling the magnetic system with steel $K_{зс} = 0{,}97$ and the voltage class $K_{зо} = (0{,}2;0{,}25;0{,}3)$, respectively, there is a linear dependence of the change in the mass index, and the advantage is practically the same (2-3%) of the twisted EMS.

The comparison of the extremes of value TF of the specified transformers in the correlations ranges of ETS values and the wrapping material (copper), has a linear dependence of the improvement of the TLI of the twisted magnetic circuits, which is (3.6-4.1%).

5. CONCLUSION

1. An analysis of the features of manufacturing EMC with a rectangular section of the rods, having different methods of manufacturing is done.

2. The analysis of calculation-optimization methods of single-phase static EMS designing is carried out. It is determined that the method of MM with TF that has universal geometric and electromagnetic controlled variables is the best in terms of universality for the determination of the TLI, and in work adopted as a basic method.

3. Using the base method, the following comparison results are obtained:

– the mass index of the single-phase twisted EMS is improved relative to the core EMS with the charged magnetic core at (2.6 ... 2.96%);

– the value index of a single-phase twisted EMS is improved relative to the core EMC with the charged magnetic core at (3.6 ... 4.1%).

4. For the first time, ranges of numerical values of the comparison of the main PTR (mass and cost) of the proposed variants of the EMF were obtained.

6. REFERENCES

1. Ермолин Н. П. Расчет трансформаторов малой мощности. Ленинград: Энергия, 1970. 190 с.

2. James H. Harlow Electric Power Transformer Engineering, 3rd cd. US CRC Press is an imprint of Taylor & Francis Group, 2012. 693p.

3. Майорец А. И. и др., Магнитопроводы силовых трансформаторов (технология и оборудование). Москва: Энергия, 1973. 272 с.

4. Flanagan W.M. Handbook of transformas design and application. Boston : Mc GrowHill, 1993. 232 p.

5. Colonel Wm.T. McLyman Transformer and Inductor Design Handbook, Fourth Edition Electrical and Computer Engineering. US, Taylor & Francis Inc , 2011. 667p.

6. MeLyman W.T. Transformer and Inductor Design Handbook. New York : Dekker, USA, 3rd edition, 2004. 533 p.

7. Ставинский А. А. Проблема и направления дальнейшей эволюции устройств электромеханики. *Електротехніка і електромеханіка*. 2004. №1. С. 57–61.

8. Белопольский И. И., Каретникова Е. И., Пикалова Л. Г. Расчет трансформаторов и дросселей малой мощности. Москва.: Альянс, 2013. 400с.

9. Садовий А.С. Варианты структур и конструктивние особенности однофазных статических индукционных устройств. *MOTROL.Commission of Motorization and Energetics in Agriculture*. 2014, Vol.16, No. 2. С 231-235.*(«Index Copernicus»)*.

10. Бальян Р. Х. Обрусник В. П. Аналитический метод геометрический оптимизации феромагнитных устройство. *Электричество*. 1979. №9. С.40–46.

11. Баев Н. Г. Трансформатор с оптимальной геометрией сердечников. *Электричество*. 1991. №2. С. 74–75.

12. Макарова А. В. Оптимальное соотношения размеров трансформаторов с магнитопроводом прямоугольного сечения. *Электротехника*. 1988. №7. С.2–6.

13. Макарова А. В Обобщённый метод оптимального проектирования трансформаторов и реакторов с прямоугольным сечением магнитопровода: автореф. дис. … канд. техн. наук: 05.09.01 / Всероссийский электротехнический институт им. В. И. Ленина. Москва, 1995. 20 с.

7. ANNEXES

Annex 1.

Results of calculations of values of controlled variables and indicators of mass and cost of a twisted shaft electromagnetic system with a rectangular section of the rods

Table 1

Mass index, r.u.	Coefficient of filling of the winding-up window, r.u.	Extreme values of controlled variables			The value of the mass index of EMS, r.u.
		a_m, r.u.	λ_0, r.u.	α_c, deg.	
P^*_{1fb}	0,2	2,232	2,087	0,876	21,986
	0,25	2,046	2,094	0,879	20,591
	0,3	1,909	2,099	0,880	19,561

Table 2

Cost index, r.u.	Coefficient of filling of the winding-up window, r.u.	ratio of winding copper and electrotechnical steel value, r.u.				
		3,5	4	4,5	5	5,5
P^*_{2fb}	0,2	40,521	43,499	46,349	49,091	51,741
	0,25	38,613	41,526	44,317	47,005	49,604
	0,3	37,204	40,069	43,817	45,464	48,026

Annex 2.

Results of calculations of controlled variables and mass and cost parameters values of planar rod electromagnetic system with a rectangular section of the cores of the charged magnetic circuit

Table 3

Mass index, r.u.	Coefficient of filling of the winding-up window, r.u.	Extreme values of controlled variables			The value of the mass index of EMS, r.u.
		a_m, r.u.	λ_0, r.u.	α_c, deg.	
P^*_{1sf}	0,2	2,204	2,205	0,819	22,586
	0,25	2,024	2,220	0,824	21,189
	0,3	1,891	2,233	0,829	20,157

Table 4

Cost index, r.u.	Coefficient of filling of the winding-up window, r.u.	ratio of winding copper and electrotechnical steel value, r.u.				
		3,5	4	4,5	5	5,5
P^*_{2sf}	0,2	42,021	45,153	48,151	51,038	53,828
	0,25	40,106	43,172	46,111	48,943	51,682
	0,3	38,692	41,710	44,605	47,396	50,097

Annex 3.

Graphical explanation of the technical level indicators of a rod electromagnetic system with a twisted and charged magnetic core numerical comparative analysis

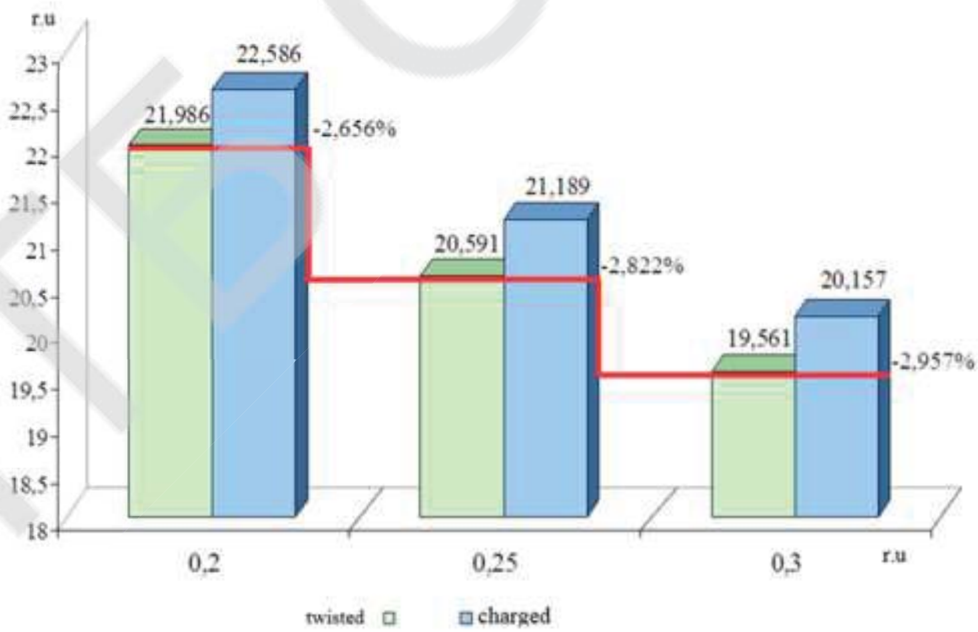

Fig. 3 Diagrams of comparison of technical level (masses) of single-phase electromagnetic systems with wired and charged magnetic circuits

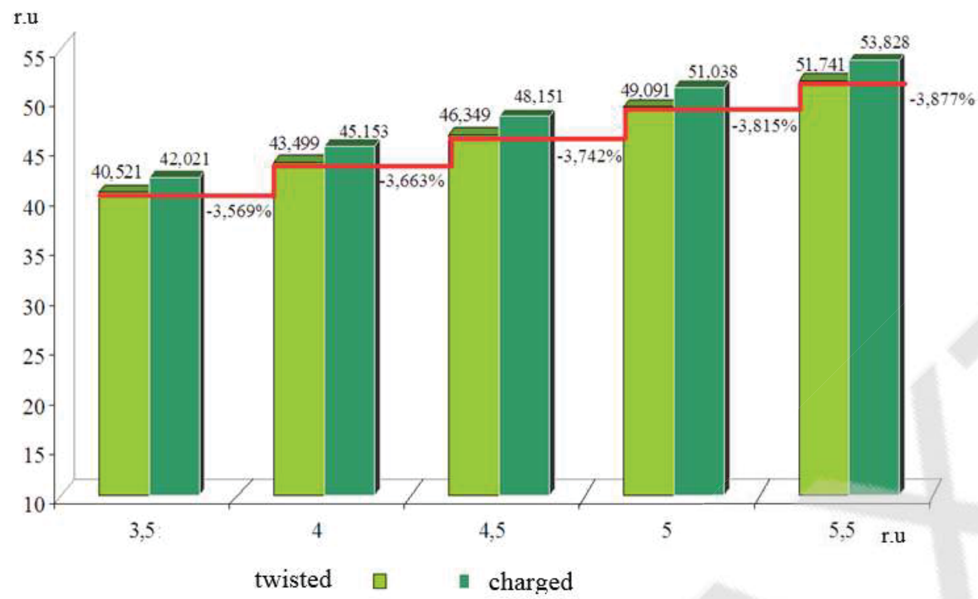

Fig. 4 Diagram of comparison of the technical level (cost) of single-phase electromagnetic systems at K_f = 0,2 r.u.

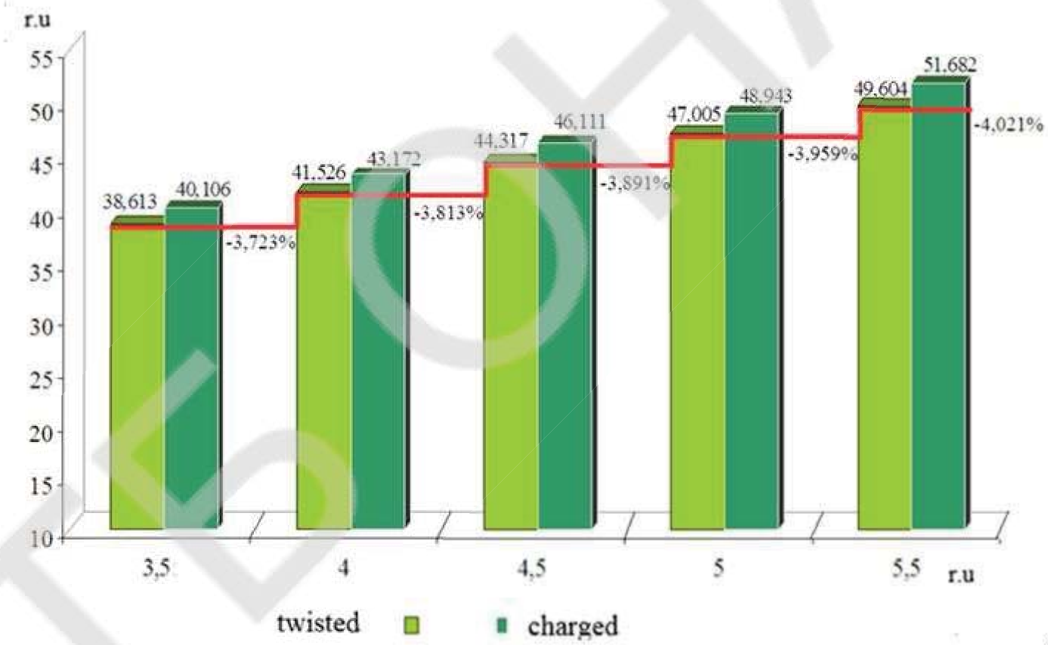

Fig. 5 Diagram of comparison of the technical level (cost) of single-phase electromagnetic systems at K_f = 0,25 r.u.

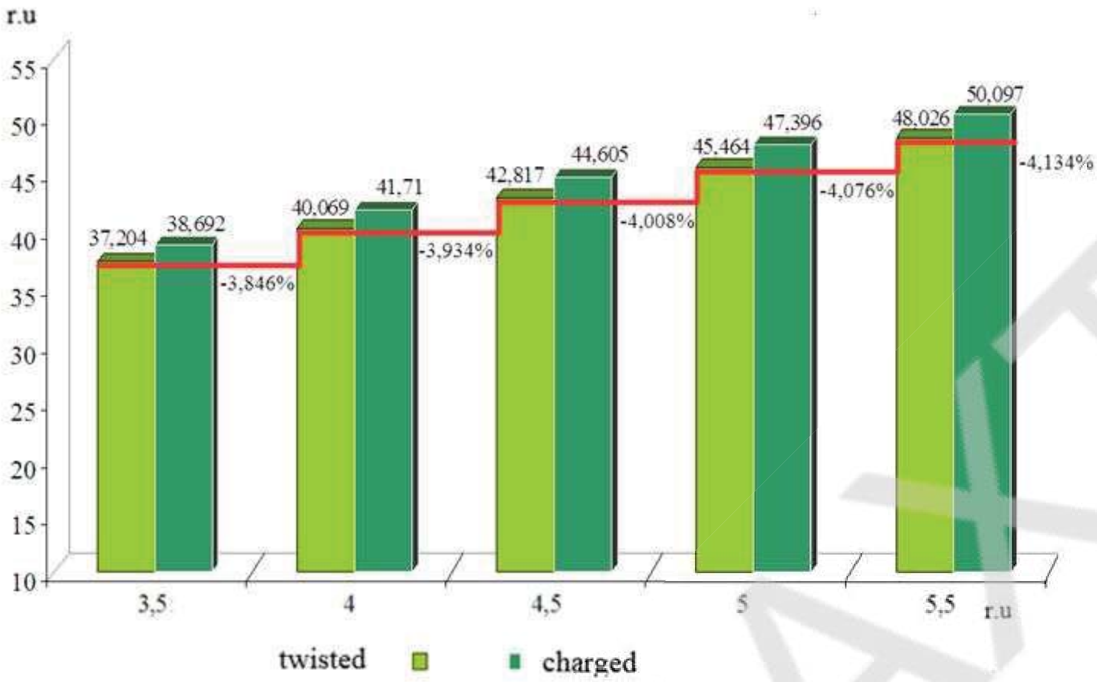

Fig. 6 Diagram of comparison of the technical level (cost) of single-phase electromagnetic systems at K_f = 0,3 r.u.